Available online at www.sciencedirect.com

ScienceDirect

IFAC Papers Online CONFERENCE PAPER ARCHIVE

IFAC-PapersOnLine 49-7 (2016) 466–471

Application of Dynamic Metabolic Flux Convex Analysis to CHO-DXB11 Cell Fed-batch Cultures

Sofia Fernandes * **Julien Robitaille** *** **Georges Bastin** ** **Mario Jolicoeur** *** **Alain Vande Wouwer** *

* *Automatic Control Laboratory, University of Mons, 31 Boulevard Dolez, 7000 Mons, Belgium (e-mail: sofia.afonsofernandes and alain.vandewouwer@umons.ac.be)*
** *Université catholique de Louvain, ICTEAM, Department of Mathematical Engineering, av. G. Lemaitre 4, B1348 Louvain-La-Neuve, Belgium (e-mail: Georges.Bastin@uclouvain.be)*
*** *Laboratory in Applied Metabolic Engineering, Department of Chemical Engineering, École Polytechnique de Montréal, C.P. 6079, Centre-ville Station, Montréal(Quebec), Canada (e-mail: Julien.Robitaille@nrc-cnrc.gc.ca and mario.jolicoeur@polymtl.ca)*

Abstract: In this work, a dynamic metabolic flux analysis based on convex analysis (DMFCA) is applied to CHO-DXB11 cell fed-batch cultures. This approach exploits all the available knowledge of the metabolic network and the time evolution of extracellular component concentrations, to determine bounded intervals for the fluxes continuously over time. Smoothing splines and mass balance differential equations are used to estimate the time evolution of the uptake and excretion rates from experimental data. Furthermore, the method is suitable for underdetermined systems, and does not require the definition of ad-hoc objective functions to be optimized. Moreover the metabolic network considered in this work allows an estimation of the carbon dioxide flux.

Keywords: CHO cells, Metabolic network, Dynamic metabolic flux analysis, Underdetermined system, Convex analysis, Mathematical modeling

1. INTRODUCTION

Over the past years, classical Metabolic Flux Analysis (MFA) has been extensively used to determine intracellular fluxes from extracellular measurements, such as cell density, substrate and product concentrations in, among others, mammalian cell cultures. This tool has been widely applied to investigate static metabolic states of cells, corresponding to intracellular fluxes which do not change over time. This assumption is supported by the observation that intracellular dynamics are much faster than extracellular dynamics. Therefore, it makes sense to neglect the fast dynamics and consider that intracellular fluxes are in pseudo-steady state (Stephanopoulos et al., 1998). The main disadvantage of classical MFA is that it does not provide information on metabolic transient. To overcome this weakness, dynamic metabolic flux analysis (DMFA) techniques have been proposed (Leighty and Antoniewicz, 2011; Lequeux et al., 2010; Llaneras et al., 2012; Niklas et al., 2011; Vercammen et al., 2014).

DMFA is also based on stoichiometric metabolite balancing within an assumed metabolic model. Most of the proposed DMFA approaches are dedicated to exactly determined or overdetermined systems. However, due to the complexity of the metabolic networks, measurable and available extracellular data is usually insufficient, leading to an underdetermined system of algebraic equations, whereby a unique solution cannot be computed. When an underdetermined system is considered, the literature suggests the use of dynamic flux balance analysis (DFBA) (Mahadevan et al., 2002) and isotopic tracer approaches for non-steady state flux analysis (Antoniewicz et al., 2007). The former approach implies the determination of an appropriate objective function, which remains valid over the whole culture, and involves large computational expenses. Detailed dynamic models including information on the kinetics have been introduced (Dorka et al., 2009; Ghorbaniaghdam et al., 2014; Robitaille et al., 2015), but those dynamic models require more experimental data for their validation. The identification of a priori unknown reaction kinetics is a critical task due to the model nonlinearity, relatively large number of parameters, and scarcity of informative experimental data.

In the present study, an alternative DMFA method is presented, which is suitable for underdetermined systems, and does not require the definition of ad-hoc objective functions. The method is based on convex analysis, and builds upon the methodology introduced in Provost and Bastin (2004) and further exploited in (Zamorano et al., 2010; Fernandes et al., 2015). In these former works the specific uptake and production rates are assumed constants and are determined using linear regression. In this

10.1016/j.ifacol.2016.07.386

study, mass balance differential equations for the extracellular concentrations, together with cubic spline smoothing, are used to assess the time evolution of the uptake and excretion rates. This information is then processed by convex analysis assuming that the intracellular species are in pseudo-steady state with respect to the time evolution of the extracellular concentrations (slow-fast approximation). Dynamic Metabolic Flux Convex Analysis (DMFCA) allows determining bounded intervals for each intracellular flux, and makes the most of the available information (metabolic network and available extracellular measurements) without introducing additional constraints or objective function. In this work, DMFCA is applied to experimental data collected from CHO fed-batch cultures.

This paper is organized as follows. The next section describes the experimental data. The considered metabolic reaction network is introduced in section 3. In section 4, the DMFCA problem is formulated, including extracellular dynamic mass balance equations, spline smoothing of the experimental data, and determination of bounded intervals for the intracellular fluxes using convex analysis. Section 5 is devoted to the numerical results and section 6 draws some conclusions.

2. EXPERIMENTAL DATA

Our study is based on a set of the experimental data from CHO-DXB11 cell line, producing a chimeric heavy chain monoclonal antibody (EG2-hFc). The experimental work has been performed at the Research Laboratory in Applied Metabolic Engineering, University of Montréal, Quebec, Canada (Robitaille et al., 2015). This set of experimental data results from a fed-batch culture and contains the time evolution of the extracellular concentrations of biomass, recombinant mAb, glucose, glutamine, lactate, alanine, ammonia and 15 amino acids (except leucine, tryptophan and cysteine). The fed-batch culture was fed daily, with punctual injections of fresh medium, to avoid nutrients limitations (see figure 1). Mathematically speaking, this type of fed-batch, with punctual injections, is characterized as a succession of batch cultures.

For more details about the experimental procedure and analytical methods, the reader is referred to Robitaille et al. (2015).

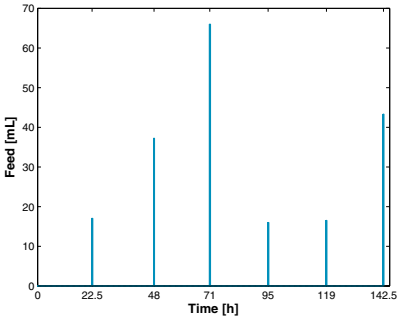

Fig. 1. Feeding strategy over CHO-DXB11 fed-batch culture.

3. METABOLIC NETWORK MODEL

The metabolic network considered in this work contains 70 biochemical reactions, 45 internal metabolites and 21 extracellular metabolites present in the culture medium, which are either substrates or products. It embraces the major reactions of central metabolism such as glycolysis, Tricarboxylic Cycle Acid (TCA), Penthose Phosphate Pathway (PPP) and amino acids metabolism (see Table 2). Furthermore, biomass and antibody synthesis are also incorporated into the model. The stoichiometric coefficients of the biomass and antibody synthesis were taken from literature (Robitaille et al., 2015).

The authors emphasize that there is no exact metabolic network to represent cellular metabolism: a candidate metabolic network is based on available metabolic knowledge and built in a way that allows describing the consumption and production of the available extracellular metabolites in a satisfactory manner. However, special care has to be exercised to preserve the stoichiometry while lumping and/or combining reactions.

Also, note that convex analysis provides positive intervals (solutions). Therefore the flux direction of the biochemical reactions is fixed a priori in agreement with the metabolic state of the cells.

Table 2. Metabolic network of CHO cells.

Flux	Reactions
	Glycolysis
v_1	$Glc_{ext} + ATP \rightarrow G6P + ADP$
v_2	$G6P \leftrightarrow F6P$
v_3	$F6P + ATP \rightarrow DHAP + G3P + ADP$
v_4	$DHAP \leftrightarrow G3P$
v_5	$G3P + NAD^+ + ADP \leftrightarrow 3PG + NADH + ATP$
v_6	$3PG + ADP \rightarrow Pyr + ATP$
	Tricarboxylic Acid Cycle
v_7	$Pyr + NAD^+ + CoASH \rightarrow AcCoA + CO_2 + NADH$
v_8	$AcCoA + Oxal + H_2O \rightarrow Cit + CoASH$
v_9	$Cit + NAD(P)^+ \rightarrow \alpha KG + CO_2 + NAD(P)H$
v_{10}	$\alpha KG + CoASH + NAD^+ \rightarrow SucCoA + CO_2 + NADH$
v_{11}	$SucCoA + GDP + Pi \leftrightarrow Succ + GTP + CoASH$
v_{12}	$Succ + FAD \leftrightarrow Fum + FADH_2$
v_{13}	$Fum \leftrightarrow Mal$
v_{14}	$Mal + NAD^+ \leftrightarrow Oxal + NADH$
	Pyruvate Fates
v_{15}	$Pyr + NADH \leftrightarrow Lac_{ext} + NAD^+$
v_{16}	$Pyr + Glu \leftrightarrow Ala + \alpha KG$
	Pentose Phosphate Pathway
v_{17}	$G6P + 2NADP^+ + H_2O \rightarrow R5P + 2NADPH + CO_2$
v_{18}	$R5P \leftrightarrow X5P$
v_{19}	$2X5P + R5P \leftrightarrow 2F6P + G3P$
	Anaplerotic Reaction
v_{20}	$Mal + NAD(P)^+ \leftrightarrow Pyr + CO_2 + NAD(P)H$
	Amino Acid Metabolism
v_{21}	$Glu + NAD(P)^+ \leftrightarrow \alpha KG + NH_4^+ + NAD(P)H$
v_{22}	$Oxal + Glu \leftrightarrow Asp + \alpha KG$
v_{23}	$Gln \rightarrow Glu + NH_4^+$
v_{24}	$Thr + NAD^+ + CoASH \rightarrow Gly + NADH + AcCoA$
v_{25}	$Ser \leftrightarrow Gly$

Flux	Reactions
v_{26}	$3PG + Glu + NAD^+ \rightarrow Ser + \alpha KG + NADH$
v_{27}	$Gly + NAD^+ \rightarrow CO_2 + NH_4^+ + NADH$
v_{28}	$Ser \rightarrow Pyr + NH_4^+$
v_{29}	$\alpha Kb + CoASH + NAD^+ \rightarrow PropCoA + NADH + CO_2$
v_{30}	$PropCoA + HCO_3^- + ATP \rightarrow SucCoA + ADP + Pi$
v_{31}	$Lys + 2\alpha KG + 3NAD(P) + FAD^+ \rightarrow \alpha Ka + 2Glu + 3NAPH + FADH_2$
v_{32}	$\alpha Ka + CoASH + 2NAD^+ \rightarrow AcetoAcCoA + 2NADH + 2CO_2$
v_{33}	$AcetoAcCoA + CoASH \rightarrow 2AcCoA$
v_{34}	$Val + \alpha KG + CoASH + 3NAD^+ + FAD^+ \rightarrow PropCoA + Glu + 2CO_2 + 3NADH + FADH_2$
v_{35}	$Ile + \alpha KG + 2CoASH + 2NAD^+ + FAD^+ \rightarrow AcCoA + Glu + CO_2 + 2NADH + FADH_2 + PropCoA$
v_{36}	$AcetoAc + SucCoA \rightarrow AcetoAcCoA + Succ$
v_{37}	$Phe + NADH \rightarrow Tyr + NAD^+$
v_{38}	$Tyr + \alpha KG \rightarrow Fum + AcetoAc + Glu + CO_2$
v_{39}	$Met + Ser + ATP \rightarrow Cys + \alpha Kb + NH_4^+ + AMP$
v_{40}	$Cys \rightarrow Pyr + NH_4^+$
v_{41}	$Asn \leftrightarrow Asp + NH_4^+$
v_{42}	$Arg \rightarrow Orn + urea$
v_{43}	$Orn + \alpha KG \leftrightarrow Glu\gamma SA + Glu$
v_{44}	$Pro \rightarrow Glu\gamma SA$
v_{45}	$Glu\gamma SA + NAD(P)^+ \rightarrow Glu + NAD(P)H$
v_{46}	$His \rightarrow Glu + NH_4^+$
v_{47}	$Orn + CarbP \rightarrow Cln$
v_{48}	$Cln + Asp + ATP \rightarrow ArgSucc + AMP$
v_{49}	$ArgSucc \rightarrow Arg + Fum$
	Biomass Synthesis
v_{50}	$0.06Ala + 0.04Arg + 0.04Asn + 0.03Asp + 0.02Gln + 0.04Glu + 0.06Gly + 0.02His + 0.09Ile + 0.06Lys + 0.01Met + 0.02Phe + 0.03Pro + 0.05Ser + 0.04Thr + 0.02Tyr + 0.04Val + 3.78ATP + 0.03G6P + 0.03R5P + 0.09Cit \rightarrow Biomass + 3.78ADP$
	Antibody Synthesis
v_{51}	$0.06Ala + 0.02Arg + 0.05Asn + 0.04Asp + 0.04Gln + 0.05Glu + 0.07Gly + 0.02His + 0.10Ile + 0.06Lys + 0.01Met + 0.04Phe + 0.07Pro + 0.11Ser + 0.11Thr + 0.03Tyr + 0.09Val + 4ATP \rightarrow mAb + 3.78ADP$
	Transport Reactions
v_{52}	$Asp_{ext} \rightarrow Asp$
v_{53}	$Asn_{ext} \rightarrow Asn$
v_{54}	$Gly \rightarrow Gly_{ext}$
v_{55}	$Ser_{ext} \rightarrow Ser$
v_{56}	$Glu \rightarrow Glu_{ext}$
v_{57}	$Tyr_{ext} \rightarrow Tyr$
v_{58}	$Ala \rightarrow Ala_{ext}$
v_{59}	$Arg_{ext} \rightarrow Arg$
v_{60}	$Gln_{ext} \rightarrow Gln$
v_{61}	$His_{ext} \rightarrow His$
v_{62}	$Ile_{ext} \rightarrow Ile$
v_{63}	$Lys_{ext} \rightarrow Lys$
v_{64}	$Met_{ext} \rightarrow Met$
v_{65}	$Phe_{ext} \rightarrow Phe$
v_{66}	$Thr_{ext} \rightarrow Thr$
v_{67}	$Val_{ext} \rightarrow Val$
v_{68}	$NH_4^+ \rightarrow NH_{4\ ext}^+$
v_{69}	$Pro_{ext} \rightarrow Pro$
v_{70}	$CO_2 \rightarrow CO_{2ext}$

4. DYNAMIC METABOLIC FLUX CONVEX ANALYSIS

The goal of DMFCA is to compute a set of admissible flux distributions continuously over time $v(t)$, using a pseudo-steady state assumption (no accumulation of internal metabolites):

$$\begin{pmatrix} N_i^{45\times 70} & 0 \\ N_m^{21\times 70} & -v_m^{21\times 1}(t) \end{pmatrix} \times \begin{pmatrix} v(t) \\ 1 \end{pmatrix} = 0 \qquad (1)$$

where N_i is the stoichiometric matrix deduced from the metabolic network, N_m is the matrix connecting the fluxes to the available measurements and v_m represents the specific uptake and excretion rates of the measured extracellular species.

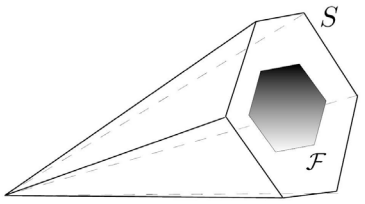

Fig. 2. Convex polyedron cones S and $\mathcal{F}$.

The metabolic network under study is not redundant ($rank(N_i) = m = 45$), and with the information provided by 21 extracellular measurements, it is an underdetermined system with a degree of freedom of 4.

4.1 Extracellular flux determination

Extracellular fluxes of the twenty-two metabolites can be computed based on their mass balance differential equations, involving cellular growth (μ), substrate uptake (υ_s) and product secretion (υ_p), as described by:

$$\frac{dX}{dt} = (\mu - D)X \qquad (2)$$

$$\frac{dS}{dt} = -DS - \upsilon_s X + DS_{in} \qquad (3)$$

$$\frac{dP}{dt} = -DP + \upsilon_p X + DP_{in} \qquad (4)$$

where X, S, P, S_{in}, P_{in} and D denote biomass, substrate, product, influent substrate and product and dilution rate, respectively. The dilution rate is defined as $D = \frac{F_{in}}{V}$, where F_{in} is the inlet feed rate and V the broth volume.

Firstly, the experimental data is smoothed off using smoothing splines and then the time derivatives appearing on the left-hand side of equations 2-4 are evaluated.

4.2 Intracellular flux determination

The set of solutions to equation 1 can be computed using convex analysis. This approach is based on the interpretation of elementary fluxes modes (simplest metabolic pathways linking substrates to products) and makes the most of the available information (i.e., metabolic network and extracellular measurements) without imposing any artificial constraint.

Geometrically speaking, the set of positive solutions to $N_i v(t) = 0$ generates a convex polyhedron cone S (see figure 2). Any flux distribution v in the cone S can be expressed as a non-negative linear combination of a set of elementary flux vectors e_i, which are the edges of the polyhedral cone S:

$$v(t) = w_1(t)e_1(t) + w_2(t)e_2(t) + \cdots + w_p(t)e_p(t), \qquad w_i(t) \geq 0 \qquad (5)$$

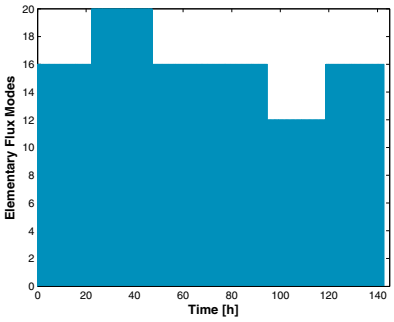

Fig. 3. Temporal evolution of the number of computed elementary flux modes.

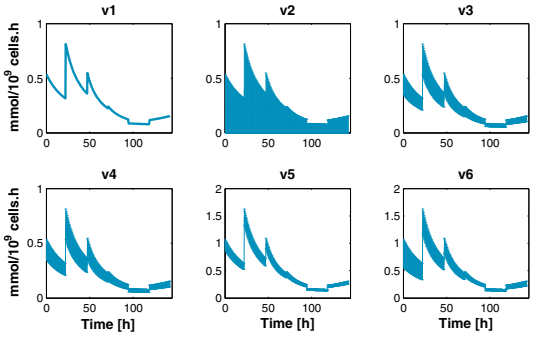

Fig. 4. Dynamic evolution of glycolysis metabolic fluxes along culture time.

If the system is further constrained with the information provided by the extracellular measurements (specific uptake and excretion rates), the solution space reduces to a convex polytope $\mathcal{F}$ in the positive orthant, where each admissible flux distribution $v(t)$ can be expressed as a convex combination of a set of non-negative basis vectors f_i which are the edges of this polytope. The set of admissible flux vectors is defined as:

$$v(t) = \sum_i w_i(t) f_i(t), \qquad w_i(t) \geq 0, \qquad \sum_i w_i(t) = 1 \quad (6)$$

The basis vectors $f_i(t)$, the so-called elementary flux vectors of the flux space $\mathcal{F}$, can be obtained applying the software METATOOL (Pfeiffer et al., 1999) to the matrix:

$$\begin{pmatrix} N_i^{45\times 70} & 0 \\ N_m^{21\times 70} & -v_m^{21\times 1}(t) \end{pmatrix} \quad (7)$$

and in turn the admissible bounds $v_j^{min}(t)$ and $v_j^{max}(t)$ for each admissible flux $v_j(t)$:

$$\begin{aligned} & v_j^{min}(t) \leq v_j(t) \leq v_j^{max}(t), \\ & \quad with \\ & v_j^{min}(t) = \min_i f_i^j(t), v_j^{max}(t) = \max_i f_i^j(t) \end{aligned} \quad (8)$$

where $f_i^j(t)$ is the j-th component of the i-th basis vector $f_i(t)$. Note that METATOOL calculates 70 650 elementary flux modes from the set of positive solutions $N_i v(t) = 0$. However, after the system being constrained with the information provided by the extracellular measurements, the number of elementary flux vectors decreases drastically. For example, at $t = 0$ only 16 elementary flux vectors are computed. Figure 3 shows the evolution of the number of elementary flux modes computed over time.

The system is said well posed if the solution set is not empty and if all the metabolic fluxes are bounded. Otherwise, the system is said to be ill posed and additional extracellular information has to be provided.

5. DMFCA IN ACTION

In this section, DMFCA is applied to the available experimental data from CHO fed-batch cultures. Recombinant mAb, glucose, glutamine, lactate, alanine, ammonia and 15 amino acids (except leucine, tryptophan and cysteine) are the extracellular available experimental data.

Note that the authors do not have access to the extracellular carbon dioxide ($CO_{2_{ext}}$). However, the metabolic network considered in this work allows an estimation of the carbon dioxide flux (more details are given in subsection 5.3).

5.1 Glycolytic fluxes

The rate of glycolysis is similar to the glucose uptake rate (see figure 4). It can also be observed that the highest flux through the glycolytic pathway occurs at early exponential phase. Indeed, in most metabolic flux studies of CHO cells, glycolytic fluxes are typically observed to be maximum at early exponential phase and are also associated with high production rates of lactate (see figure 5: flux v_{15}) (Ahn and Antoniewicz, 2013; Templeton et al., 2013).

5.2 Tricarboxylic Acid cycle

According to the DMFCA results, the major nutrient flux for the TCA cycle is glucose-derived pyruvate (v_6). The pyruvate generated from glycolysis can be metabolized via lactic acid fermentation to be reduced to lactate, can participate in the synthesis of alanine or enter in the TCA cycle to be oxidized to CO2. From figure 5 one can see that, in the first 95 hours, pyruvate is channeled mainly towards lactate (phenomenon characterized as Warburg effect (Vazquez et al., 2010)); while in the last 45 hours, the majority of pyruvate is channeled into TCA cycle via pyruvate dehydrogenase (v_7) flux to be oxidized to CO_2, meaning that most of the pyruvate is used to obtain energy by means of the cellular respiration. This high pyruvate dehydrogenase (PDH) complex activity was also found in other studies of mammalian cells metabolism (Ahn and Antoniewicz, 2013; Sheikholeslami et al., 2014).

5.3 Pentose phosphate pathway

The PPP is the pathway used by the cells to synthesize the precursors of nucleic acids (DNA and RNA) and reducing power in the form of NADPH.

Several studies have demonstrated that the G6P is mostly converted to pyruvate by glycolysis and in less quantities by PPP either in hybridoma or CHO cells (Ahn and

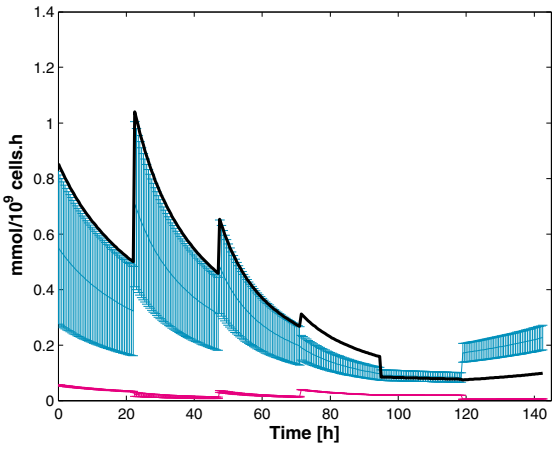

Fig. 5. Dynamic evolution of pyruvate fates along culture time. Turquoise: Pyruvate entering TCA cycle v_7. Black: Pyruvate reduced to lactate v_{15}. Magenta: Pyruvate reduced to alanine v_{16}.

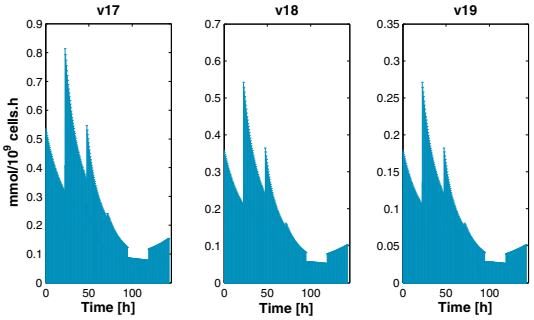

Fig. 6. Dynamic evolution of PPP metabolic fluxes determined by DMFCA.

Antoniewicz, 2011; Sengupta et al., 2011). However, in this study, comparing metabolic fluxes v_2 and v_{17} one can observe that there is no difference between the conversion of G6P to pyruvate by glycolysis (figure 4) and by PPP (figure 6). This is explained by the fact that Glycolysis and PPP are set in parallel, and thus are not distinguishable from extracellular measurements only. The assimilation of G6P could occur in the Glycolysis or in the PPP indistinctly, and thus their flux intervals are in counterbalance.

5.4 Amino acid metabolism

A simple way to determine which amino acid is the main contributor to antibody production is to calculate the ratio between essential amino acid uptake rate and the corresponding stoichiometric coefficient for antibody synthesis. The lowest the ratio, the more that given amino acid contributes to antibody production. The average ratios are depicted in figure 7, from which it appears that the amino acid valine is the most significant contributor to antibody production. Concerning the conditionally or non-essential amino acids (aspartate, glycine, serine, glutamate, alanine, arginine and asparagine) they can be consumed or synthesized according to the cell needs.

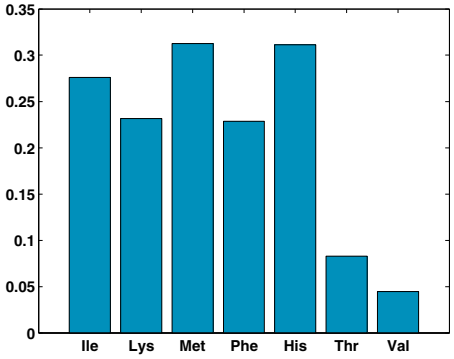

Fig. 7. Ratio (in average) between essential amino acids uptake rate and its stoichiometry for cellular antibody.

5.5 Estimation of carbon dioxide flux

Carbon dioxide is difficult to measure and is seldom an available measurement (Frahm et al., 2002). Looking at cellular metabolism we can note that carbon dioxide participates in several pathways and, therefore it would be interesting and in some cases necessary to have access to this measurement. For instance, in previous works by the same authors (Zamorano et al., 2010; Fernandes et al., 2015), an estimate of the CO_2 measurement had to be borrowed from the literature in order to solve the system of equations. This happened due to the presence of some elementary paths linking non-measured inputs to non-measured outputs. To solve the problem it was necessary to identify which were the unmeasured extracellular metabolites participating in these paths and add them to the set of extracellular measurements. From the global reaction deduced from the elementary flux modes, it appeared that either $CO_{2_{ext}}$ or urea were the extracellular species in question and one of them had to be measured.

With the metabolic network considered in the present work and the available extracellular measurements an estimation of the carbon dioxide flux can be achieved since proline, which participates in urea cycle, can be measured. However, the estimated carbon dioxide flux appears larger than the values reported in (Gray et al., 1996; Lovrecz and Gray, 1994). An interpretation of this result is difficult in view of the different experimental conditions (particularly the variation of the dilution rate in the experiment considered in the present study).

6. CONCLUSION

In this study, the dynamic metabolism of fed-batch CHO cell culture is achieved, using a new approach: a dynamic metabolic flux analysis based on convex analysis (positive algebra). This method allows the determination of bounded intervals for the intracellular metabolic fluxes continuously over the culture time. The main advantage of the proposed procedure is that it does not require additional constraints or objective functions, and provides relatively narrow intervals for the intracellular metabolic fluxes.

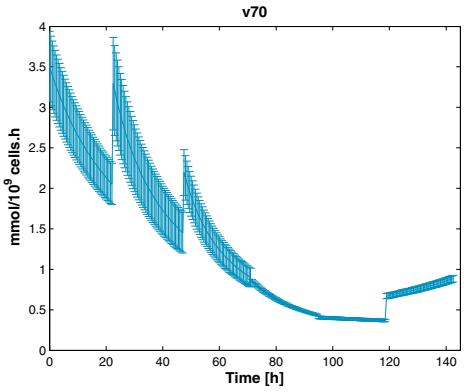

Fig. 8. Dynamic evolution of CO_2 flux determined by DMFCA.

ACKNOWLEDGEMENTS

This paper presents research results of the Belgian Network DYSCO (Dynamical Systems, Control, and Optimization), funded by the Interuniversity Attraction Poles Programme initiated by the Belgian Science Policy Office.

REFERENCES

Ahn, W.S. and Antoniewicz, M.R. (2011). Metabolic flux analysis of CHO cells at growth and non-growth phases using isotopic tracers and mass spectrometry. *Metabolic engineering*, 13(5), 598–609.

Ahn, W.S. and Antoniewicz, M.R. (2013). Parallel labeling experiments with [1, 2-13 C] glucose and [U-13 C] glutamine provide new insights into CHO cell metabolism. *Metabolic engineering*, 15, 34–47.

Antoniewicz, M.R., Kraynie, D.F., Laffend, L.A., González-Lergier, J., Kelleher, J.K., and Stephanopoulos, G. (2007). Metabolic flux analysis in a nonstationary system: fed-batch fermentation of a high yielding strain of E. coli producing 1, 3-propanediol. *Metabolic engineering*, 9(3), 277–292.

Dorka, P., Fischer, C., Budman, H., and Scharer, J.M. (2009). Metabolic flux-based modeling of mAb production during batch and fed-batch operations. *Bioprocess and biosystems engineering*, 32(2), 183–196.

Fernandes, S., Bastin, G., and Vande Wouwer, A. (2015). Metabolic Flux Analysis of Hybridoma Cells: Underdetermined Network and Influence of Batch and Perfusion Operating Modes. In *Mathematical Modelling*, volume 8, 464–469.

Frahm, B., Blank, H.C., Cornand, P., Oelßner, W., Guth, U., Lane, P., Munack, A., Johannsen, K., and Pörtner, R. (2002). Determination of dissolved CO 2 concentration and CO 2 production rate of mammalian cell suspension culture based on off-gas measurement. *Journal of biotechnology*, 99(2), 133–148.

Ghorbaniaghdam, A., Chen, J., Henry, O., and Jolicoeur, M. (2014). Analyzing clonal variation of monoclonal antibody-producing CHO cell lines using an in silico metabolomic platform. *PloS one*, 9(3).

Gray, D.R., Chen, S., Howarth, W., Inlow, D., and Maiorella, B.L. (1996). CO2 in large-scale and high-density CHO cell perfusion culture. *Cytotechnology*, 22(1-3), 65–78.

Leighty, R.W. and Antoniewicz, M.R. (2011). Dynamic metabolic flux analysis (DMFA): a framework for determining fluxes at metabolic non-steady state. *Metabolic engineering*, 13(6), 745–755.

Lequeux, G., Beauprez, J., Maertens, J., Van Horen, E., Soetaert, W., Vandamme, E., and Vanrolleghem, P.A. (2010). Dynamic metabolic flux analysis demonstrated on cultures where the limiting substrate is changed from carbon to nitrogen and vice versa. *BioMed Research International*, 2010.

Llaneras, F., Sala, A., and Picó, J. (2012). Dynamic estimations of metabolic fluxes with constraint-based models and possibility theory. *Journal of Process Control*, 22(10), 1946–1955.

Lovrecz, G. and Gray, P. (1994). Use of on-line gas analysis to monitor recombinant mammalian cell cultures. *Cytotechnology*, 14(3), 167–175.

Mahadevan, R., Edwards, J.S., and Doyle, F.J. (2002). Dynamic flux balance analysis of diauxic growth in Escherichia coli. *Biophysical journal*, 83(3), 1331–1340.

Niklas, J., Schräder, E., Sandig, V., Noll, T., and Heinzle, E. (2011). Quantitative characterization of metabolism and metabolic shifts during growth of the new human cell line AGE1. HN using time resolved metabolic flux analysis. *Bioprocess and biosystems engineering*, 34(5), 533–545.

Pfeiffer, T., Nu, J., Montero, F., Schuster, S., et al. (1999). METATOOL: for studying metabolic networks. *Bioinformatics*, 15(3), 251–257.

Provost, A. and Bastin, G. (2004). Dynamic metabolic modelling under the balanced growth condition. *Journal of Process Control*, 14(7), 717–728.

Robitaille, J., Chen, J., and Jolicoeur, M. (2015). A Single Dynamic Metabolic Model Can Describe mAb Producing CHO Cell Batch and Fed-Batch Cultures on Different Culture Media. *PloS one*, 10(9), e0136815.

Sengupta, N., Rose, S.T., and Morgan, J.A. (2011). Metabolic flux analysis of CHO cell metabolism in the late non-growth phase. *Biotechnology and bioengineering*, 108(1), 82–92.

Sheikholeslami, Z., Jolicoeur, M., and Henry, O. (2014). Elucidating the effects of postinduction glutamine feeding on the growth and productivity of CHO cells. *Biotechnology progress*, 30(3), 535–546.

Stephanopoulos, G., Aristidou, A.A., and Nielsen, J. (1998). *Metabolic engineering: principles and methodologies*. Academic press.

Templeton, N., Dean, J., Reddy, P., and Young, J.D. (2013). Peak antibody production is associated with increased oxidative metabolism in an industrially relevant fed-batch CHO cell culture. *Biotechnology and bioengineering*, 110(7).

Vazquez, A., Liu, J., Zhou, Y., and Oltvai, Z.N. (2010). Catabolic efficiency of aerobic glycolysis: the Warburg effect revisited. *BMC systems biology*, 4(1), 58.

Vercammen, D., Logist, F., and Van Impe, J. (2014). Dynamic estimation of specific fluxes in metabolic networks using non-linear dynamic optimization. *BMC systems biology*, 8(1), 132.

Zamorano, F., Vande Wouwer, A., and Bastin, G. (2010). A detailed metabolic flux analysis of an underdetermined network of CHO cells. *Journal of biotechnology*, 150(4), 497–508.